JOURNAL OF GUIDANCE, CONTROL, AND DYNAMICS
Vol. 32, No. 2, March–April 2009

Engineering Notes

ENGINEERING NOTES are short manuscripts describing new developments or important results of a preliminary nature. These Notes should not exceed 2500 words (where a figure or table counts as 200 words). Following informal review by the Editors, they may be published within a few months of the date of receipt. Style requirements are the same as for regular contributions (see inside back cover).

Collision-Geometry-Based Pulsed Guidance Law for Exoatmospheric Interception

Ashwini Ratnoo* and Debasish Ghose†
Indian Institute of Science, Bangalore 560012, India

DOI: 10.2514/1.37863

I. Introduction

In THE absence of aerodynamic control forces, divert thrusters are used to generate lateral acceleration required by interceptors in exoatmospheric engagements. The thrusters can be fired as pulses of constant lateral acceleration magnitude. The pulse width or duration is determined by the guidance law used.

Several guidance laws based on the zero-effort miss (ZEM) have been proposed in the literature for exoatmospheric engagements. A ZEM-based midcourse guidance law for intercepting strategic targets and spacecraft is proposed by Newman [1,2]. Later, Hablani [3] proposed a ZEM-based pulsed guidance law with image processing delays for the endgame phase. Hablani [4] also demonstrated that zero-effort-miss guidance is superior to proportional navigation guidance in the endgame phase of an exoatmospheric interception using divert thrusters. Miss distance analysis of ZEM guidance with respect to various measurement errors is carried out by Hablani and Pearson [5]. Zarchan [6] has derived the ZEM-based pulsed guidance implemented with equally spaced pulses. ZEM can be calculated from the instantaneous line-of-sight rate, the closing velocity, and the time to go. Lateral distance traveled by the interceptor depends on the width of the divert thruster pulse, which can be evaluated by equating the lateral distance to the ZEM. Because of the assumptions involved, interception cannot be guaranteed by firing a single pulse even for exact ZEM calculations. Subsequent pulses are fired to achieve a satisfactory miss distance.

In this Note, an interceptor endgame pulsed guidance law is derived by attempting to attain the collision heading rather than negating ZEM. It is shown that this strategy is more effective than ZEM-based guidance for intercepting targets with higher heading angles off the nominal head-on case. The interceptor and the target are assumed to be constant speed lag free point masses. A planar engagement scenario is considered, assuming that the interceptor can perform uncoupled guidance commands in two perpendicular planes. The proposed guidance law, to determine the pulse width, is derived in steps by 1) obtaining the collision heading based on the collision triangle engagement geometry and parameters, and 2) computing the width of the pulse fired by the divert thruster to attain the collision heading.

In the existing pulsed guidance laws, the pulses are fired either at fixed intervals [6] or every time the line-of-sight rate (or zero-effort miss) crosses a predefined threshold value [3]. In the present work, it is shown that firing pulses in quick succession results in minimum pulse widths and hence minimum control effort for interception.

For comparative study, the derivation of pulsed guidance [6], based on ZEM steering, is described briefly in Sec. II. The proposed guidance law is derived in Sec. III, followed by some results on pulse firing sequence in Sec. IV. Simulation studies are carried out in Sec. V.

II. Zero-Effort-Miss Steering

Zero-effort miss is defined as the distance by which the interceptor would miss the target if the target continued along its present course and the interceptor made no further corrective maneuvers. There are two ways of evaluating ZEM, and we describe them in brief here.

A. Zero-Effort Miss Using Exact Nonlinear Model

Consider a planar engagement geometry as shown in Fig. 1a. The exact expression for time to go t_{go} in a planar engagement is derived by Rawling [7] as

$$t_{go} = \frac{-R\dot{R}}{(\dot{R}^2 + R^2\dot{\theta}^2)} \tag{1}$$

where R and θ are current range and line-of-sight angle, respectively. Time to go is the time-until-minimum separation, assuming both the interceptor and the target as nonmaneuvering. The exact expression for the minimum separation or the virtual miss distance R_{vm} in such a scenario is (see Rawling [8])

$$R_{vm} = \frac{R^2\dot{\theta}}{\sqrt{(\dot{R}^2 + R^2\dot{\theta}^2)}} \tag{2}$$

The component of R_{vm} normal to the line of sight (see Fig. 1a) is $R\dot{\theta}t_{go}$ where $R\dot{\theta}$ is the relative target velocity normal to the line of sight. The exact value of ZEM $= R_{vm}$ and ZEM $= R\dot{\theta}t_{go}$ can be considered as an approximation [3–6].

B. Zero-Effort Miss Using Trajectory Linearization

ZEM can also be evaluated using trajectory linearization [6] in the following way

$$\mathrm{ZEM}_{lin} = V_c\dot{\theta}t_{golin}^2 \tag{3}$$

where

$$t_{golin} = \frac{-R}{\dot{R}} \tag{4}$$

$$V_c = -\dot{R} \tag{5}$$

Using Eqs. (4) and (5) in Eq. (3), we have

Received 3 April 2008; revision received 8 December 2008; accepted for publication 8 December 2008.

*Graduate Student, Department of Aerospace Engineering; jmk@aero.iisc.ernet.in.

†Professor, Department of Aerospace Engineering; dghose@aero.iisc.ernet.in.

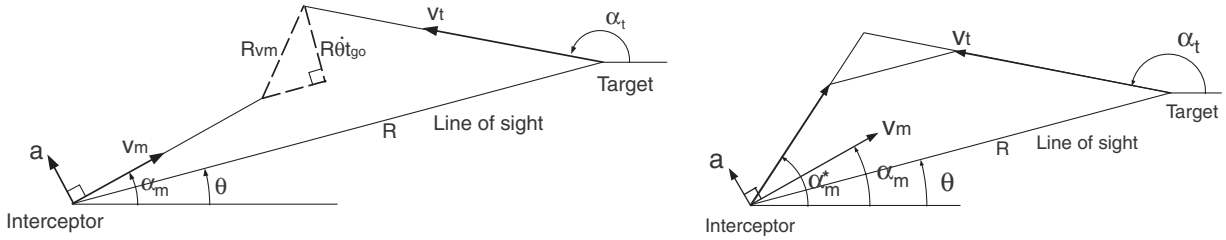

a) Zero effort miss using rawling's virtual miss **b) Collision course**

Fig. 1 Engagement geometries.

$$\text{ZE M}_{\text{lin}} = R\dot{\theta}t_{\text{golin}} = \frac{-R^2\dot{\theta}}{\dot{R}} \tag{6}$$

It can be readily seen that the values of t_{golin} and ZEM_{lin} are greater than Rawling's t_{go} and R_{vm} given by Eqs. (1) and (2), respectively [7,8]. Also, the assumptions involved in trajectory linearization are untenable for higher heading angles off the nominal head-on collision course.

Consider a divert pulse of magnitude a fired for Δt s, as shown in Fig. 2. The lateral distance z_{pulse} traveled by the interceptor by firing a pulse of width Δt is given as

$$z_{\text{pulse}} = \tfrac{1}{2}a\Delta t^2 + a\Delta t(t_{\text{go}} - \Delta t) \tag{7}$$

For successful interception of the target, the distance traveled by the interceptor due to the divert pulse is equated to ZEM, that is,

$$\tfrac{1}{2}a\Delta t^2 + a\Delta t(t_{\text{go}} - \Delta t) = \text{ZEM} \tag{8}$$

Solving for Δt,

$$\Delta t = t_{\text{go}}\left[1 - \sqrt{1 - \frac{2\text{ZEM}}{at_{\text{go}}^2}}\right] \tag{9}$$

For real solutions of Eq. (9), we have

$$\frac{2\text{ZEM}}{at_{\text{go}}^2} \le 1 \tag{10}$$

If $2\text{ZEM}/at_{\text{go}}^2 > 1$, then the interceptor lateral acceleration capability is not enough to annul ZEM. To achieve the minimum possible miss distance $\Delta t = t_{\text{go}}$ is assumed in such cases.

The t_{go} given by Eq. (1) is based on the fact that both the interceptor and the target are nonmaneuvering, which is not true after closing the guidance loop. Consequently, even with Rawling's ideal point mass nonlinear model for ZEM calculation [8], one pulse is not enough and subsequent pulses have to be fired for achieving the desired miss.

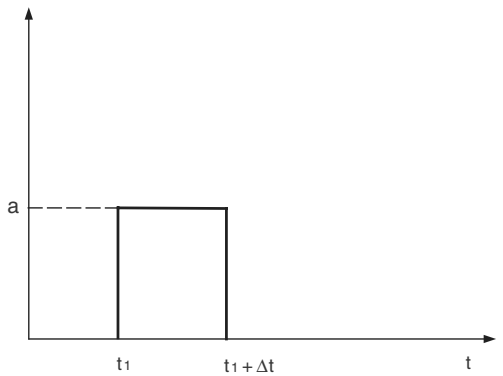

Fig. 2 Lateral acceleration pulse.

III. Collision Course Steering

The problem of pulse guidance can be viewed from a collision course approach, as shown in Fig. 1b. Here α_m^* denotes the desired heading for the interceptor to be on the collision course with a nonmaneuvering target, and α_m denotes the instantaneous interceptor heading. We determine the pulse duration that guides the interceptor to the desired heading.

For the interceptor to be on the collision course, the line-of-sight rate needs to be zero, that is,

$$\dot{\theta} = \left(\frac{1}{R}\right)[v_m \sin(\alpha_m^* - \theta) - v_t \sin(\alpha_t - \theta)] = 0 \tag{11}$$

$$\Rightarrow \alpha_m^* = \theta + \sin^{-1}\left\{\frac{v_t \sin(\alpha_t - \theta)}{v_m}\right\} \tag{12}$$

We know that

$$v_t \sin(\alpha_t - \theta) = v_m \sin(\alpha_m - \theta) + R\dot{\theta} \tag{13}$$

From Eqs. (12) and (13), we have

$$\alpha_m^* = \theta + \sin^{-1}\left\{\sin(\alpha_m - \theta) + \frac{R\dot{\theta}}{v_m}\right\} \tag{14}$$

The interceptor turn rate $\dot{\alpha}_m$ and pulse magnitude a are related as

$$v_m\dot{\alpha}_m = a \tag{15}$$

Integrating Eq. (15) for a pulse duration, we get

$$\Delta t = (\alpha_m^* - \alpha_m)\frac{v_m}{a} \tag{16}$$

From Eqs. (14) and (16), we have

$$\Delta t = \frac{v_m}{a}\left[\sin^{-1}\left\{\sin(\alpha_m - \theta) + \frac{R\dot{\theta}}{v_m}\right\} - (\alpha_m - \theta)\right] \tag{17}$$

where a has the same sign as $\dot{\theta}$, that is,

$$a = \begin{cases} >0 & \text{if } \dot{\theta} > 0 \\ <0 & \text{if } \dot{\theta} < 0 \end{cases} \tag{18}$$

Equation (17) gives the proposed guidance strategy for the pulse duration, considering the target to be nonmaneuvering. The guidance law involves interceptor speed, interception heading, current range, and line-of-sight rate which are available onboard.

For real solutions of Eq. (17), we must have

$$\left\{\sin(\alpha_m - \theta) + \frac{R\dot{\theta}}{v_m}\right\} \le 1 \tag{19}$$

If $\{\sin(\alpha_m - \theta) + (R\dot{\theta}/v_m)\} > 1$, then the interceptor speed is not enough for a collision course to exist. The engagement geometry for such cases is shown in Fig. 3. Here, irrespective of its heading, the

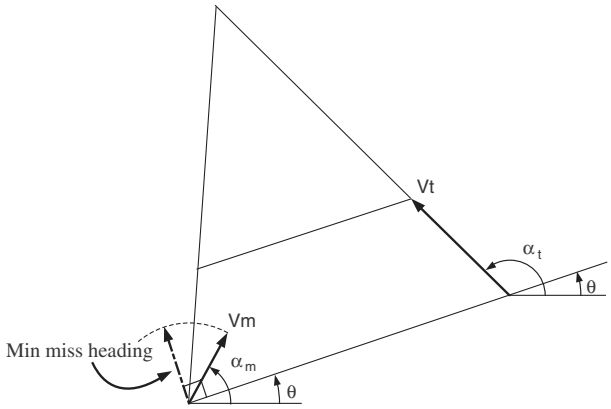

Fig. 3 No-collision geometry.

interceptor cannot be on the collision course since $v_m < v_t \sin(\alpha_t - \theta)$. To reach to the minimum possible miss distance, $\{\sin(\alpha_m - \theta) + (R\dot{\theta}/v_m)\} = 1$ is taken in such cases. The interceptor is steered to move perpendicular to the line of sight (see Fig. 3) and hence achieve the least possible miss distance. Equation (10) shows that ZEM-based steering, theoretically, annuls any ZEM by a suitable choice of a. However, as shown in Fig. 3, there are geometries for which Eq. (19) is violated and the target cannot be intercepted. Although such high heading angles off the nominal head-on case are not encountered in typical exoatmospheric engagements, it highlights a lacuna in the ZEM-based approach.

IV. Pulse Firing Sequence

In the analysis for the proposed guidance law, it is assumed that the interceptor will be maneuvered instantaneously on application of the pulse without any significant change in engagement geometry, which also implies that Δt is small. However, initial pulse durations can be high due to high heading angles off the nominal head-on case. This will require more pulses to be fired subsequently. There are several logics of pulse firing sequence existing in literature. The pulses can be equally spaced in time [6] or can be fired every time the line-of-sight rate (or zero-effort miss) crosses a threshold value [4]. The following propositions show that firing pulses with minimum delay results in least control effort.

Proposition 1: In the absence of any control force, and with $\dot{R} < 0$, the magnitude of the line-of-sight rate ($|\dot{\theta}|$) increases monotonically with time from the initial nonzero value $\dot{\theta}_0$.

Proof: Let

$$v_r = \dot{R} = v_t \cos(\alpha_t - \theta) - v_m \cos(\alpha_m - \theta) \tag{20}$$

$$v_\theta = R\dot{\theta} = v_t \sin(\alpha_t - \theta) - v_m \sin(\alpha_m - \theta) \tag{21}$$

Differentiating v_r and v_θ with respect to time, with $\dot{\alpha}_m = \dot{\alpha}_t = 0$ for unguided flight, we have

$$\dot{v}_r = \dot{\theta}\{v_t \sin(\alpha_t - \theta) - v_m \sin(\alpha_m - \theta)\} = \dot{\theta} v_\theta \tag{22}$$

$$\dot{v}_\theta = -\dot{\theta}\{v_t \cos(\alpha_t - \theta) - v_m \cos(\alpha_m - \theta)\} = -\dot{\theta} v_r \tag{23}$$

From Eqs. (20), (21), and (23), we obtain

$$\frac{\mathrm{d}}{\mathrm{d}t}(R\dot{\theta}) = -\dot{\theta}\dot{R} \Rightarrow R\ddot{\theta} = -2\dot{\theta}\dot{R} \Rightarrow \ddot{\theta} = \frac{-2\dot{R}}{R}\dot{\theta} \tag{24}$$

With $\dot{R} < 0$ and $R > 0$, we have

$$\Rightarrow \ddot{\theta} = \begin{cases} >0 & \text{if } \dot{\theta}_0 > 0 \\ <0 & \text{if } \dot{\theta}_0 < 0 \end{cases} \Rightarrow |\dot{\theta}| > 0 \tag{25}$$

Proposition 2: Pulse width Δt is a monotonically increasing function of line-of-sight rate $|\dot{\theta}|$.

Proof: Using Eq. (17),

$$\frac{\mathrm{d}\Delta t}{\mathrm{d}\dot{\theta}} = \frac{v_m}{a}\frac{\mathrm{d}}{\mathrm{d}\dot{\theta}}\left[\sin^{-1}\left\{\sin(\alpha_m - \theta) + \frac{R\dot{\theta}}{v_m}\right\} - (\alpha_m - \theta)\right] \tag{26}$$

$$= \frac{R}{a\sqrt{1 - \{\sin(\alpha_m - \theta) + (R\dot{\theta}/v_m)\}^2}} \tag{27}$$

We have $\{\sin(\alpha_m - \theta) + (R\dot{\theta}/v_m)\} < 1$ for all real values of Δt. Using Eq. (18) in Eq. (27),

$$\frac{\mathrm{d}\Delta t}{\mathrm{d}\dot{\theta}} = \begin{cases} >0 & \text{if } \dot{\theta} > 0 \\ <0 & \text{if } \dot{\theta} < 0 \end{cases} \Rightarrow \left|\frac{\mathrm{d}\Delta t}{\mathrm{d}\dot{\theta}}\right| > 0 \tag{28}$$

From Proposition 1, we see that line-of-sight rate will build up monotonically after a pulse is fired if the pulse fired does not bring the interceptor in perfect collision course with the target. As a consequence, the next pulse width required to steer the interceptor on the collision course, as proved in Proposition 2, will also increase monotonically with time.

The preceding results show that the pulses should be fired in quick succession to minimize the fuel requirement and achieve a low miss distance. In the implementation of the proposed guidance law, we assume a minimum gap of one guidance cycle time between the pulses.

V. Simulation Results

In the simulation studies, we consider the endgame phase of a high-speed exoatmospheric engagement. The target is approximately 3–5 times faster than the interceptor. The minimum pulse width of the side thruster is 15 ms and the guidance cycle is taken to be 0.2 s. One guidance cycle is taken as the minimum separation in time between any two consecutive pulses. If a commanded pulse has a magnitude less than the minimum pulse width, then the line-of-sight rate is allowed to build up until the pulse width required becomes equal to the minimum pulse width and then the pulse is fired.

We assume that, at the beginning of the endgame, the interceptor points toward the target (with $\alpha_{m0} = \theta_0 = 0$). The nominal case is a head-on engagement with the target pointing directly toward the interceptor with $\alpha_t = 180$ deg.

A. Capturability with Respect to Target Heading

In this case study, we compare the performance of the proposed guidance law with the ZEM-based pulsed guidance law given by Eq. (9), where ZEM is the component of Rawling's virtual miss distance normal to the line of sight, that is, ZEM $= R\dot{\theta}t_{\mathrm{go}}$ [8]. Here, a fixed number of three pulses are fired.

First, we assume target and interceptor speeds to be 4000 m/s and 1000 m/s, respectively, with an initial separation of 50 km. The pulse acceleration magnitude is taken as 200 m/s^2. We vary the target heading angle over the nominal head-on case and evaluate the performance of the guidance law in terms of the miss distance. We choose $\alpha_t = 174$ deg for the first set of simulations, which is 6 deg off the nominal head-on case. The engagement ends in a successful interception with a miss distance of 0.0199 m when the proposed guidance law is used. The corresponding pulse profile is shown in Fig. 4a. The first pulse is of maximum width, followed by the second one after one guidance cycle. The third pulse is the smallest one and is fired when the command given by Eq. (17) crosses the minimum pulse width of 15 ms. Line-of-sight variation with time is plotted in Fig. 4b. The line-of-sight rate is forced toward zero by the first pulse with some residual error. The error starts building up after the first pulse is fired and the second pulse reduces it to a still lower value. The same effect continues in the third pulse. Near to interception, the line-

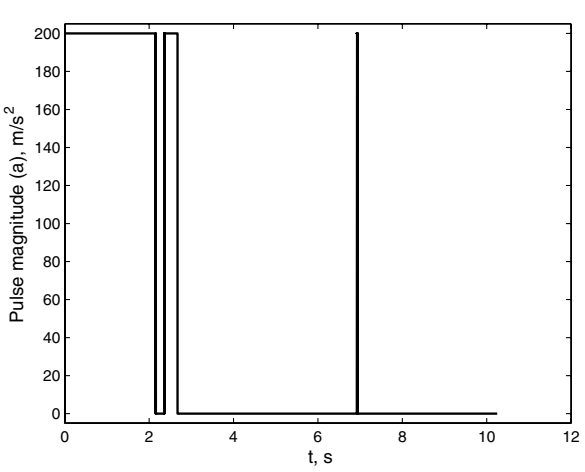

a) Pulse profile

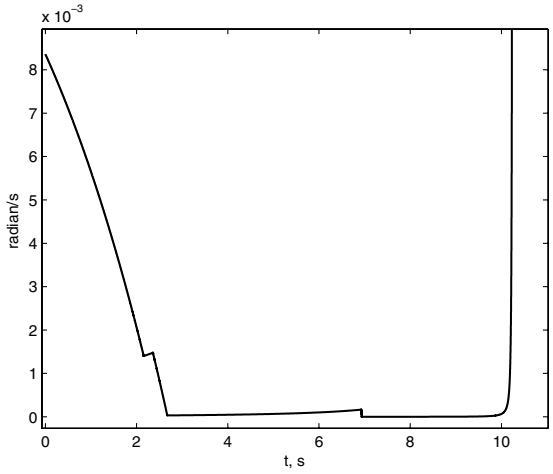

b) Line-of-sight rate vs time

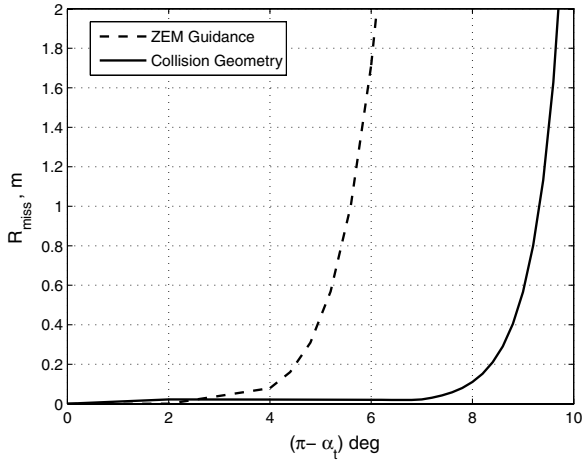

c) Miss distance vs target heading angle off the nominal head-on

Fig. 4 Results for case 4.

of-sight rate increases rapidly as the range tends to zero. As shown in Fig. 4c, we vary the target heading angle over the nominal head-on case and show that the guidance law is effective over a range of ± 9.7 deg over the nominal for an acceptable miss distance of 2 m. Figure 4c also shows the result for ZEM-based guidance law, which is effective over a range of ± 6.1 deg. Thus, the proposed guidance law shows an improvement of almost 60%. The results are listed as case 1 in the first row of Table 1.

The effect of the initial closing range on the performance of the proposed guidance law is investigated in cases 2 and 3. Results (see Table 1) show that the relative performance of the proposed guidance law improves with increasing closing range. The collision heading guidance law pulse width given by Eq. (17) is independent of the closing range since $R\dot{\theta}$ depends only on target and interceptor velocity components normal to the line of sight, as observed in Eq. (13). However, for a given pulse width, the change in engagement geometry during firing of a pulse is higher for a closer range, and so the performance improves as the closing range increases.

The effect of closing speed on the performance of the proposed guidance law is investigated in cases 4 and 5, as listed Table 1. For the proposed guidance law, an increased closing velocity induces more changes in the collision geometry during firing of a pulse, thus deteriorating the performance. Nevertheless, the proposed guidance law captures a wider range of target headings as compared to the ZEM-based guidance law.

Both the guidance laws considered here have a strong relationship with the magnitude of the pulse acceleration a [see Eqs. (9) and (17)]. Cases 6 and 7 in Table 1 are simulated with $a = 180$ and 150 m/s^2, respectively. The reduced value of a for the proposed guidance law results in a higher pulse width for a given target heading angle off the nominal head-on case. A wider pulse causes more changes in the

Table 1 Engagement parameters and results

Case	v_m, m/s	v_t, m/s	x_{t0}, km	a, m/s^2	$(\pi - \alpha_t)$ for $R_{\text{miss}} = 2$ m, proposed	$(\pi - \alpha_t)$ for $R_{\text{miss}} = 2$ m, ZEM law
1	1000	4000	50	200	9.6989 deg	6.1194 deg
2	1000	4000	75	200	11.9418 deg	5.9485 deg
3	1000	4000	100	200	12.5212 deg	5.7878 deg
4	1000	5000	50	200	6.7474 deg	4.8944 deg
5	1000	6000	50	200	4.9891 deg	4.0533 deg
6	1000	4000	50	180	8.9911 deg	6.0644 deg
7	1000	4000	50	150	7.7826 deg	5.951 deg
8	2000	5000	100	200	9.1171 deg	8.484 deg

collision geometry during the firing of a pulse, resulting in higher miss distance.

Case 8 in Table 1 is simulated with an increased interceptor speed of 2000 m/s. Again, results show better performance by the proposed guidance law.

B. Miss Distance Study with Different Pulse Separations

Here, we study the effect of delay between two pulses on the performance of the proposed guidance law. Time separation between the pulses is taken as integer multiples of guidance cycles, that is, 1,2,4, and 8 guidance cycles. The delay is represented by n_g as the number of guidance cycles. Three target headings at $\alpha_t = 171$, 172, and 174 deg are considered and the results are listed in Table 2. For $\alpha_t = 174$ deg, the miss distance is less than 0.0241 m and is not much affected by varying the separation between the pulses. The pulse widths, as claimed in Proposition 2, increase with increased separation between them. The divert velocity requirement calculated as $\Delta V = \int |a| \mathrm{d}t$ also increases with increasing pulse separation. Similar trends are observed for $\alpha_t = 172$ deg with the maximum miss distance of 0.9352 for $n_g = 8$. For increased target heading angle with respect to the nominal, $\alpha_t = 171$ deg and $n_g = 8$, the proposed guidance has a large miss distance of 6.7898 m. Results for the ZEM-based guidance scheme, with similar trends in pulse widths and divert velocity requirements, show higher miss distances, as shown in Table 3. The values in parentheses are obtained by using ZEM $= R_{\mathrm{vm}}$ (see Fig. 1a). This exact expression of ZEM does improve the performance, but not significantly. The simulation studies in this section concur with the claim in Propositions 1 and 2 that minimum time separation between the pulses results in minimum control effort and lower miss distance.

C. Simulations with Higher Number of Pulses

To study the divert velocity ΔV requirements for a given miss, we relax the constraint on the number of pulses and compare the proposed guidance law with the ZEM-based guidance law. Here, we consider one guidance cycle time separation between the consecutive pulses, that is, $n_g = 1$. Also, n_p represents the number of pulses fired in an engagement. For simulations with the proposed guidance law, we consider $\alpha_t = 171$ deg and 172 deg. The results are shown in Table 4. Results show that an $R_{\mathrm{miss}} \leq 0.017$ m is obtained using four pulses. The results for ZEM guidance with the same engagement parameters are shown in Table 5. The ZEM-based guidance law requires seven and eight pulses, respectively, for intercepting the target with $\alpha_t = 172$ and 171 deg. The corresponding divert velocity requirements and miss distance is also higher as compared with the proposed guidance law. Again, results in parentheses of Table 5 obtained using the exact expression ZEM $= R_{\mathrm{vm}}$ show improvement in the performance, but not significantly. The simulation results in this section show superiority of the proposed guidance law over the ZEM-based guidance law in terms of number of pulses fired and divert velocity requirements.

Table 2 Proposed guidance with three pulses

α_t	n_g	Δ_1, s	Δ_2, s	Δ_3, s	$\sum_{i=1}^{3} \Delta_i$, s	$\Delta V = \int \lvert a \rvert \mathrm{d}t$, m/s	R_{miss}, m
174 deg	1	2.1568	0.3143	0.0150	2.4861	497.22	0.0199
	2	2.1568	0.3226	0.0150	2.4944	498.88	0.0200
	4	2.1568	0.3407	0.0150	2.5125	502.50	0.0198
	8	2.1568	0.3833	0.0165	2.5566	511.32	0.0241
172 deg	1	2.9520	0.6871	0.0381	3.6772	735.44	0.1098
	2	2.9520	0.7074	0.0433	3.7027	740.54	0.1420
	4	2.9520	0.7522	0.0571	3.7613	752.26	0.2447
	8	2.9520	0.8606	0.1128	3.9254	785.08	0.9352
171 deg	1	3.3804	1.005	0.0930	4.4784	895.68	0.5668
	2	3.3804	1.0377	0.1074	4.5255	905.10	0.7504
	4	3.3804	1.1909	0.1476	4.7189	943.78	1.3896
	8	3.3804	1.2867	0.3371	5.0042	1000.8	6.7898

Table 3 Zero-effort-miss guidance with three pulses

α_t	n_g	Δ_1, s	Δ_2, s	Δ_3, s	$\sum_{i=1}^{3} \Delta_i$, s	$\int \lvert a \rvert \mathrm{d}t$, m/s	R_{miss}, m
174 deg	1	2.3728	0.0881	0.0150	2.4759	495.18	1.6721
		(2.3825)	(0.0792)	(0.0150)	(2.4767)	(495.34)	(1.5101)
	2	2.3728	0.0905	0.0150	2.4783	495.66	1.6758
		(2.3825)	(0.0813)	(0.0150)	(2.4788)	(495.77)	(1.5131)
	4	2.3728	0.0957	0.0150	2.4835	496.70	1.6839
		(2.3825)	(0.0860)	(0.0150)	(2.4835)	(496.70)	(1.5196)
	8	2.3728	0.1081	0.0162	2.4971	499.42	1.7040
		(2.3825)	(0.0972)	(0.0150)	(2.4946)	(498.93)	(1.5353)
172 deg	1	3.3458	0.2461	0.0561	3.6480	729.60	17.0713
		(3.3722)	(0.2246)	(0.0516)	(3.6485)	(729.69)	(15.7092)
	2	3.3458	0.2538	0.0600	3.6596	731.92	17.1695
		(3.3722)	(0.2316)	(0.0551)	(3.6589)	(731.78)	(15.7900)
	4	3.3458	0.2706	0.0697	3.6861	737.22	17.3872
		(3.3722)	(0.2470)	(0.0639)	(3.6831)	(736.62)	(15.9733)
	8	3.3458	0.3122	0.1028	3.7608	752.16	17.9654
		(3.3722)	(0.2851)	(0.0943)	(3.7515)	(750.30)	(16.4579)
171 deg	1	3.8897	0.3883	0.1220	4.4000	880.00	47.4838
		(3.9307)	(0.3582)	(0.1136)	(4.4025)	(880.50)	(44.2744)
	2	3.8897	0.4016	0.1317	4.4230	884.60	47.9058
		(3.9307)	(0.3702)	(0.1224)	(4.4233)	(884.66)	(44.6280)
	4	3.8897	0.4310	0.1563	4.4770	895.40	48.8714
		(3.9307)	(0.3973)	(0.1451)	(4.4731)	(894.62)	(45.4540)
	8	3.8897	0.5059	0.2514	4.6470	929.40	51.6327
		(3.9307)	(0.4664)	(0.2326)	(4.6297)	(925.95)	(47.8095)

Table 4 Proposed guidance with higher number of pulses

α_t	n_p	$\sum \Delta$, s	$\Delta V = \int \lvert a \rvert \mathrm{d}t$, m/s	R_{miss}, m
172 deg	4	3.6922	738.4400	0.0170
171 deg	4	4.4932	898.6400	0.0146

Table 5 Zero-effort-miss guidance with higher number of pulses

α_t	n_p	$\sum \Delta$, s	$\Delta V = \int \lvert a \rvert \mathrm{d}t$, m/s	R_{miss}, m
172 deg	7	3.7080	741.6000	0.0589
		(3.7085)	(741.7030)	(0.0542)
171 deg	8	4.5023	900.4506	0.2375
		(4.5018)	(900.3620)	(0.2214)

VI. Conclusions

A collision-course-based pulsed guidance law is proposed for planar exoatmospheric engagements. Nonlinear engagement geometry is considered for deriving the collision heading and hence the pulse width required to steer the interceptor on the collision course. The proposed law requires line-of-sight and interceptor parameters for implementation and is independent of time to go. It is shown, for a general pulsed guidance scenario, that pulses should be fired in quick succession for minimum divert acceleration and hence minimum divert velocity requirement. Simulations show superior miss distance and divert velocity requirement performance as compared with the ZEM-based guidance law. The results presented here are of a preliminary nature. Future work could include a dynamic model for the interceptor and a maneuvering target together with noisy measurements.

References

[1] Newman, B., "Strategic Intercept Midcourse Guidance Using Modified Zero Effort Miss Steering," *Journal of Guidance, Control, and Dynamics*, Vol. 19, No. 1, Jan.–Feb. 1996, pp. 107–112. doi:10.2514/3.21586

[2] Newman, B., "Spacecraft Intercept Guidance Using Zero Effort Miss Steering," *AIAA Guidance, Navigation and Control Conference*, AIAA TP A93-51301 22-63, Pt. 3, 1993, pp. 1707–1716.

[3] Hablani, H. B., "Pulsed Guidance of Exoatmospheric Interceptors with Image Processing Delays in Angle Measurements," *AIAA Guidance, Navigation and Control Conference*, AIAA Paper No. 2000-4272: AAO-37107, 2000.

[4] Hablani, H. B., "Endgame Guidance and Relative Navigation of Strategic Interceptors with Delays," *Journal of Guidance, Control, and Dynamics*, Vol. 29, No. 1, Jan.–Feb. 2006, pp. 82–94. doi:10.2514/1.12748

[5] Hablani, H. B., and Pearson, D. W., "Determination of Guidance Parameters of Exo-Atmospheric Interceptors via Miss Distance Error Analysis," *AIAA Guidance, Navigation and Control Conference and Exhibit*, AIAA Paper No. 2001-4279:A01-37145, 2001.

[6] Zarchan, P., *Tactical and Strategic Missile Guidance*, 4th ed., Vol. 199, AIAA, Reston, VA, 2002, pp. 342–352.

[7] Rawling, A. G., "Passive Determination of Homing Time," *AIAA Journal*, Vol. 6, No. 8, Aug. 1968, pp. 1604–1606. doi:10.2514/3.4826

[8] Rawling, A. G., "On Nonzero Miss Distance," *Journal of Spacecraft and Rockets*, Vol. 6, No. 1, 1969, pp. 81–83. doi:10.2514/3.29539